Magnetic order in RMn_2Ge_2 (R=Y,Ca) compounds and their solid solutions with $LaMn_2Ge_2$

S. Di Napoli,[1] A. M. Llois,[1,2] G. Bihlmayer,[3] and S. Blügel[3]
[1]*Departamento de Física, Facultad de Ciencias Exactas y Naturales, Universidad de Buenos Aires, 1428 Buenos Aires, Argentina*
[2]*Departamento de Física, Comisión Nacional de Energía Atómica, Avenida del Libertador 8250, 1429 Buenos Aires, Argentina*
[3]*Institut für Festkörperforschung, Forschungszentrum Jülich, D-52425 Jülich, Germany*
(Received 6 November 2006; published 12 March 2007)

We present a systematic study of the stability of the collinear and noncollinear magnetic states of RMn_2Ge_2 (R=Y,Ca) compounds as a function of the lattice parameter so as to simulate alloying with La, using density-functional theory calculations. The results allow us to discriminate between chemical and structural factors that determine the magnetic properties of these systems. We find that, to a large extent, the magnetic moments are determined by the interatomic Mn-Mn distance, given by the size of the substitutional atom. We also find that the different magnetic structures appearing along the phase diagrams are to be mainly ascribed to the interstitial electronic density related to the divalent or trivalent character of the R atom.

DOI: 10.1103/PhysRevB.75.104406 PACS number(s): 75.25.+z, 75.50.−y, 75.30.Ds, 72.80.Ga

I. INTRODUCTION

A large variety of interesting phenomena is reported for compounds crystallizing in the $ThCr_2Si_2$ structure: among them, the Mn family RMn_2X_2 (where R is a di-or trivalent ion and X=Si,Ge) shows especially rich magnetic phase diagrams with different types of antiferromagnetic or noncollinear orders on the Mn sublattice (see, e.g., Ref. 1 and references therein). If R is a magnetic rare-earth ion, at lower temperatures long-range magnetic order is possible also on the rare-earth sublattice. If R is nonmagnetic, there are two possibilities how this ion can influence the magnetism: (i) via the size of the ion R (e.g., by substituting the large La by the small Y), which changes the lattice parameters and thereby the Mn-Mn distance, or (ii) by changing its chemical valency (e.g., by alloying Ca with a La compound) and thereby the valence electron concentration in the system. A change of chemical valency can also be triggered by the ion X, e.g., in $EuMn_2Si_2$ the rare-earth ion is trivalent while in $EuMn_2Ge_2$ it is divalent.[2] The magnetic order can be shown to change in solid solutions of these two compounds as a function of the Si or Ge concentration. But in all these studies, it is difficult to separate the effects (i) and (ii), since every change of the chemical composition is also accompanied by a change of the lattice parameters. A deeper understanding of the underlying mechanisms that influence the magnetic order in this class of materials is desirable not only for academic purposes, but might also prove useful for the design of materials with specific magnetic properties.

Using neutron-diffraction studies, a large variety of magnetic ground states has been reported in systems of the type $R_{(1-x)}Z_xMn_2Ge_2$ (R,Z=Y,La,Ca). These compounds also crystallize in the $ThCr_2Si_2$ structure. The Mn-Mn distances in these structures are mainly determined by the size of the other atoms building the compound. The Mn sublattice forms a simple tetragonal framework and the Mn-Mn interlayer distance along the c axis, $R^c_{\text{Mn-Mn}}$, is between 5.4 and 5.6 Å, whereas the Mn-Mn intralayer distance, $R^a_{\text{Mn-Mn}}$, lies in the range 2.8–3.2 Å, being nearly half the one corresponding to $R^c_{\text{Mn-Mn}}$. Typically, for a given pair of R and Z, the Mn-Mn interlayer distance is almost constant while the intralayer distance varies with the concentration x. The magnetic phase diagrams of $La_{(1-x)}Y_xMn_2Ge_2$ (Ref. 3) and $La_{(1-x)}Y_xMn_2Si_2$ (Ref. 4) show interesting similarities as a function of concentration, which leads to attempts to classify the magnetic phases as a function of the lattice parameters of the Mn subsystem alone. However, in the La-rich part of the phase diagram differences can also be observed, namely, the presence of spin spirals in the germanide systems.

At low temperatures, as a function of increasing concentration, both series go from ferromagnetic (FM) canted structures to antiferromagnetic (AFM) collinear ones passing through antiferromagnetic canted phases. Apart from the (noncollinear) canted spinstructures, also spiral (conical) spin-density waves as magnetic ground states can be realized. At higher temperatures, the magnetic structures show intraplane as well as interplane antiferromagnetism, going over to just interplane antiferromagnetism with increasing values of x. We have already explored in a previous contribution[5] the underlying chemical differences of $LaMn_2Ge_2$ and $LaMn_2Si_2$ by performing first-principles calculations. While the probably most significant effect on the magnetism could be traced back to a change of the lattice parameter when substituting Ge by Si, we found additional effects due to the change in the hybridization of the more covalent Si to which the differences in the magnetic structure could be attributed.

The phase diagram of $La_{(1-x)}Ca_xMn_2Ge_2$ (Ref. 6) clearly shows a rapid succession of variations in the magnetic ground state, since the trivalent La ion is substituted by the divalent Ca. In other words, in this series the introduction of small amounts of Ca (a small variation of x away from 0) induces several magnetic transitions. In contrast to the (La,Y) system, these transitions occur without a very large change in the lattice parameters, so that we can attribute them mainly to a change of valence electron concentration by the chemical modification.

To separate chemical from structural effects induced by the substitutions, we study the relative stabilities of various magnetic structures of the compounds RMn_2Ge_2 (R=Y,Ca) as a function of the lattice parameter, simulating alloying with La to form solid solutions of increasing concentration,

by doing first-principles calculations. In this contribution we do not attempt to calculate the full phase diagram (including temperature effects), but estimate from the relative stability of the calculated magnetic structures their order of occurrence as temperature increases and compare with the experiments. We also study the chemical effect on the value of the magnetic moments of the studied compounds as a function of the valence character of the substituting atoms.

After a short presentation of the calculational method in Sec. II, we review the experimental facts (Sec. III) before we present the first-principles results and a discussion in Sec. IV.

II. METHOD OF CALCULATION

The calculations are performed in the framework of the vector spin-density functional theory[8] in the local-density approximation as formulated by Moruzzi *et al.*[9] Earlier calculations[5,10] have shown that the use of a generalized gradient approximation for the exchange-correlation potential in the case of noncollinear structures generally does not lead to satisfactory results, since it overestimates the stability of antiferromagnetic states. We used the FLEUR code,[11] which is an implementation of the full-potential linearized augmented plane-wave method[12] that allows the treatment of noncollinear magnetism including incommensurate spin spirals.[13,14]

In our calculations on YMn_2Ge_2, the **k**-point set used corresponds to 100 **k** points in the irreducible wedge of the Brillouin zone (IBZ). The tetragonal magnetic unit cell contains ten atoms. In the case of $CaMn_2Ge_2$, we used 343 **k** points in the IBZ as we considered a body centered tetragonal unit cell containing only five atoms. The different magnetic orders were introduced as spin spirals, with high-symmetry points chosen as ordering vectors of the spiral. In both series of compounds, the calculations were performed with a plane-wave cutoff, K_{max}, of 3.4 a.u.$^{-1}$ leading to 85–95 basis functions per atom, depending on the lattice parameters. The convergence of the energies with respect to these quantities has been carefully checked. The number of **k** points and K_{max} were chosen in such a way as to ensure convergence of total energy differences of 10^{-3} eV. The muffin-tin radii have been set to 2.3 a.u. for all atoms in the case of $CaMn_2Ge_2$ and to 2.2 a.u. for all atoms in the case of YMn_2Ge_2.

III. REVIEW OF EXPERIMENTAL RESULTS

Let us first review the experimental results obtained for the magnetic ground states of the solid solutions $La_{1-x}Ca_xMn_2Ge_2$,[6] $La_{1-x}Y_xMn_2Ge_2$,[3] and $La_{1-x}Y_xMn_2Si_2$.[4] At all concentrations the $ThCr_2Si_2$ structure of these compounds is maintained and the volume changes are primarily caused by a change in the in-plane lattice constant a of the tetragonal unit cell or the c/a ratio, respectively.

In the case of $La_{(1-x)}Y_xMn_2X_2$ (X=Si,Ge), at the Y-rich side of the phase diagrams (small in-plane lattice parameter a), a structure with in-plane ferromagnetically coupled Mn atoms and an antiferromagnetic interlayer coupling is formed (AFil, also denoted as AFM3 in Ref. 5). As the La content increases, both the silicide and the germanide transform into a canted antiferromagnetic structure, AFmc (see Fig. 1). This structure is obtained by tilting the magnetic moments of the AFil structure as indicated in Fig. 1. Further expansion of the lattice constant (i.e., moving to the La-rich side) induces an additional conical spin spiral in the germanide, leading to the AFmi structure and, after this, to the Fmi one, i.e., the interplane coupling changes to ferromagnetic. In the silicide, the sequence of transitions as a function of growing in-plane lattice constant is AFil, AFmc, Fmc, and Fmi, i.e., first the interplane coupling changes to ferromagnetic, then the spin spiral sets in.

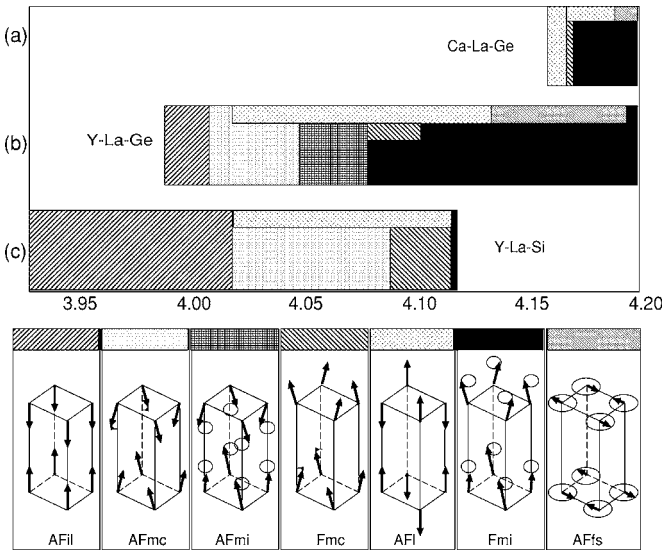

FIG. 1. Schematic representation of the experimentally determined phases of $La_{1-x}Ca_xMn_2Ge_2$ (a), $La_{1-x}Y_xMn_2Ge_2$ (b), and $La_{1-x}Y_xMn_2Si_2$ (c). The phases are ordered according to the in-plane lattice constant (in Å), which is proportional to the La concentration. The evolution with temperature is shown vertically. At the bottom of the figure, the magnetic structures of the Mn atoms for the AFil, AFmc, and AFmi types are represented. The Fmc and Fmi structures are similar to the AFmc and AFmi ones, but with a ferromagnetic interplane coupling. For a canting angle of 90°, the Fmc and AFmc structures are equivalent to the AFl ordering. The AFfs (flat spiral) structure is similarly obtained from the AFmi (or Fmi) with a 90° semicone angle. The Fml structure (also called AFM2 in Ref. 5, not shown here) is similar to the AFl but with a ferromagnetic interplane coupling.

If La is substituted by Ca in the $LaMn_2Ge_2$ structure, the Fmi ordering is maintained in a wide concentration range before it crosses (for large Ca concentrations) over to a small region of stability of the Fmc structure and, finally, the AFl (also called AFM1 in Ref. 5) magnetic order sets in. The AFl is a collinear state that can be obtained from the AFmc structure with a canting angle of 90°. It is interesting to note that at higher temperatures the $La_{1-x}Y_xMn_2Ge_2$ and $La_{1-x}Y_xMn_2Si_2$ systems also show a concentration range where the AFl ordering is stable; additionally in $La_{1-x}Y_xMn_2Ge_2$, for intermediate temperatures, a region of stability for the Fmc structure can be observed, approximately in the range of in-plane lattice constants where the Fmc structure is stable in the corresponding silicide. Both the Ca and the Y germanide show, at higher temperatures and

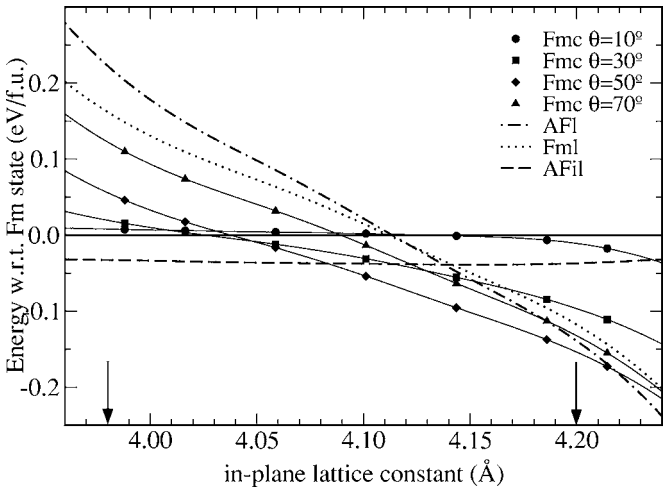

FIG. 2. Total energy per formula unit of different magnetic configurations of YMn_2Ge_2 as a function of the in-plane lattice parameter. The energies are given with respect to the ferromagnetic state. The lattice parameter c has been kept fixed at the experimental value for $LaMn_2Ge_2$, i.e., 10.97 Å. Arrows indicate the lattice parameters of YMn_2Ge_2 (3.98 Å) and $LaMn_2Ge_2$ (4.20 Å).

larger lattice constants, a flat-spiral structure that can be obtained from the AFmi one with a semicone angle of 90° (AFfs).

IV. RESULTS AND DISCUSSION

As mentioned in the Introduction, we simulate the phase diagrams of RMn_2Ge_2 (R=Y,Ca) and their solid solutions with La by calculating the evolution of the total energies and Mn magnetic moments with increasing value of the lattice constant for different magnetic structures of these compounds.

A. YMn_2Ge_2

In $La_{1-x}Y_xMn_2Ge_2$, when going from YMn_2Ge_2 to $LaMn_2Ge_2$, the lattice parameter c expands only by 1.1%, while a changes by 5.3%. Therefore, we keep in the calculations c constant and compare the total energies of various magnetic structures of YMn_2Ge_2 as a function of the in-plane lattice constant. Referencing all energies to the ferromagnetic state (Fig. 2), we see that for the experimental in-plane lattice parameter (a=3.98 Å) the AFil state has the lowest energy, in good agreement with experimental data. The AFil state is always about 35 meV/f.u. lower in energy than the Fm state, and this energy difference corresponds to the exchange coupling between the two (ferromagnetic) Mn planes in the unit cell. Considering only collinear states, we observe at in-plane lattice constants larger than 4.14 Å a transition to the AFl state, indicating that at a Mn-Mn distance of 2.93 Å the in-plane antiferromagnetic order gets more stable than the in-plane FM structure. At this point, a FM interplane coupling is energetically less favorable, but we observed that for smaller lattice constants (a<4.11 Å) and in-plane AFM ordering, a FM interplane order is preferred [E(Fml) <E(AFl), where the Fml structure is the one with in-plane antiferromagnetic coupling and ferromagnetic between planes].

Allowing also for noncollinear, canted magnetic Fmc structures, we observed that in a region between a=4.08 and 4.22 Å, a Fmc structure with a canting angle of about 50° is lower in energy than the other collinear ones. Indeed, such a magnetic configuration with an additional spin spiral (Fmi) is also found experimentally as the ground state for $La_{1-x}Y_xMn_2Ge_2$ in the range where the in-plane lattice parameter is between 4.08 and 4.20 Å (see Fig. 1).

If we compare the results for YMn_2Ge_2 at 4.20 Å with our previous results on $LaMn_2Ge_2$,[5] we see that also in the La compound the energy difference between Fm and AFil state is 37 meV/f.u., and the AFl state is 220 meV lower in energy than the Fm one (150 meV in YMn_2Ge_2 at 4.20 Å). In YMn_2Ge_2, the Fml structure is higher in energy than the AFl; in $LaMn_2Ge_2$, it is the other way round. In the latter compound, inclusion of spin spirals in the calculations can lower the total energies of the Fmc states by about 22 meV, which made then finally the ground state; in the Y compound, the Fmc state is already lower in energy than any collinear state.

Experimentally, for lattice constants between 4.01 and 4.05 Å, a canted antiferromagnetic structure with a canting angle lying in the range 25°–34° is observed. Therefore, we also calculated YMn_2Ge_2 for a few lattice constants in the AFmc structure and found that, at least for a canting angle of 35° and a lattice constant of about 4.04 Å, the AFmc structure gets lower in energy than the AFil one. Although we have not calculated additional spin spirals, we expect from our experience in previous calculations of $LaMn_2Ge_2$ (see preceding paragraph) that around this lattice constant, there is a region where the AFmi configurations give the ground state.

Summarizing, we obtain from the calculations a sequence of magnetic ground-state structures (AFil, AFmc/AFmi, and Fmc/Fmi with increasing in-plane lattice constant), which is in line with the experimental results.

B. $CaMn_2Ge_2$

When we study how the different magnetic structures depend on the lattice parameter in the case of $CaMn_2Ge_2$, as summarized in Fig. 3, we notice considerable differences as compared to the Y compound. In this system, the AFl structure (antiferromagnetism between and in the planes) is the most stable of the selected ones for all calculated lattice constants, although the stability decreases with decreasing Mn-Mn distance. At the experimental in-plane lattice constant of 4.16 Å, the AFl ordering is by far the most stable magnetic structure and, even experimentally, no other magnetic order is observed up to the Néel temperature. Expanding this lattice constant further toward the experimental lattice constant of $LaMn_2Ge_2$ (4.20 Å), the energy difference with respect to the Fmc structures increases even more, so that we can safely exclude pure geometrical effects to be responsible for the transition to the Fmc phase that is observed in experiment.[6] Let us remember that the ground state of $LaMn_2Ge_2$ is of the Fmi type.[7] This trend continues also if

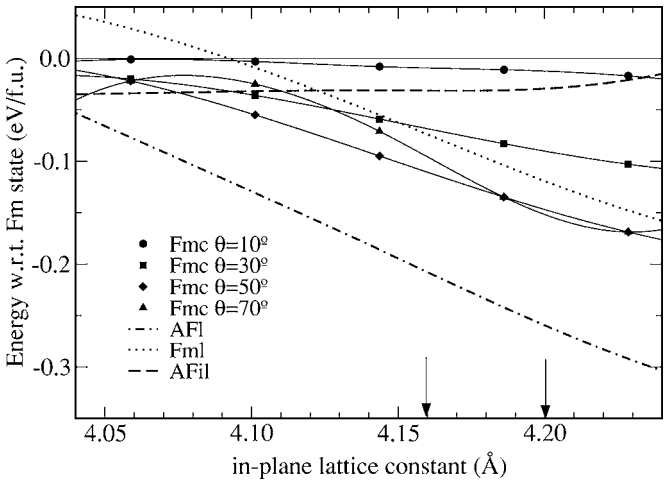

FIG. 3. Total energy per formula unit of different magnetic configurations of $CaMn_2Ge_2$ as a function of the in-plane lattice parameter. The energies are referenced to the ferromagnetic state. The lattice parameter c has been kept fixed at the experimental value for $CaMn_2Ge_2$, i.e., 10.82 Å. Indicated are the lattice parameters of $CaMn_2Ge_2$ (4.16 Å) and $LaMn_2Ge_2$ (4.20 Å).

we go to even larger lattice constants, like that of $BaMn_2Ge_2$, 4.44 Å, where the AFl ordering is still the lowest in energy. This kind of magnetic order has also been observed experimentally in this compound.[15]

Apart from these apparent differences between YMn_2Ge_2 and $CaMn_2Ge_2$, there are also wide similarities among the total energy curves of Figs. 2 and 3, for instance, the energy difference between the Fm and AFil states is about 35 meV and, quite constant in both cases, the crossing between the AFil and Fml states occurs at 4.14 and 4.12 Å in the Y and Ca compound, respectively; the crossover from the AFil to the 50° Fmc state appears at around 4.08 Å in both cases. The main difference lies in the AFl structure, which is significantly more stable in the Ca compound than in the corresponding YMn_2Ge_2. While in Y compound the interaction between the Mn planes is weak for an in-plane antiferromagnetic structure, in the Ca compound it is of the order of 100 meV. This is a factor of 3 larger than for in-plane ferromagnetically ordered structures. Like in YMn_2Ge_2, with increasing in-plane lattice constant the stability of the antiferromagnetic order increases, indicating that large Mn moments and a low electronic density in the interstitial region act in favor of antiferromagnetic coupling between the planes.

C. Magnetic moments

The most obvious source for differences between YMn_2Ge_2 and $CaMn_2Ge_2$ is, of course, the fact that Y is a trivalent ion, while Ca is divalent and, therefore, donates less electrons than the Y ion. This change in the chemical composition is, of course, also accompanied with a structural change of the lattice, most prominently reflected in the in-plane lattice constant, which is 3.98 Å for YMn_2Ge_2 and is 4.16 Å for $CaMn_2Ge_2$, while the c lattice constant changes by only about 0.02 Å. The magnetic moments will be affected by both the valency of the constituting ions and the resulting structure. To separate these two influences, we compare the magnetic moments of the La, Y, and Ca compounds at the same in-plane lattice parameter (4.06 Å) and for the same magnetic structure in Table I. We find that the reduction of valence electrons results in just a small increase in the values of the magnetic moment of the order of $0.03-0.11\mu_B$. Actually, the extra electron of Y and La (with respect to Ca) sits mainly in the nearly nonpolarized interstitial region, thereafter slightly affecting the magnetic moments of the Mn atoms. From the density of states, we see that the majority spin Mn subbands in $CaMn_2Ge_2$ are already filled, so that additional valence electrons result in a decrease of the magnetic moment. A similar effect can explain the decrease of Mn magnetic moment when substituting Y with La: the more electropositive La ion donates more electrons to the Mn than the Y one, therefore further reducing the magnetic moment. On the other hand, the stronger covalent bonding of Si in $LaMn_2Si_2$ as compared to Ge in the germanide has been shown to result in a smaller magnetic moment in the Si compound than in the Ge one.[5]

TABLE I. Comparison between the calculated Mn magnetic moments (in units of μ_B) for different magnetic structures in four different compounds calculated at the same in-plane lattice parameter of 4.06 Å.

	μ_{Mn} (μ_B)			
State	$LaMn_2Si_2$	$LaMn_2Ge_2$	YMn_2Ge_2	$CaMn_2Ge_2$
Fm	2.03	2.14	2.16	2.27
AFil	2.08	2.19	2.19	2.27
Fml	2.67	2.77	2.71	2.74
AFl	2.70	2.77	2.74	2.80

The dominant factor determining the magnetic moments comes actually from the in-plane magnetic order and from the lattice constants. Of course, in the experiment it is not strictly possible to separate the chemical role of the di- or trivalent ion (Ca, Y, or La) from its influence on the lattice parameters. Our calculations allow us now to study separately the effects of the structure on the magnetic moment: In Fig. 4 we plot the magnetic moments of a given compound as a function of (in-plane) lattice parameter. We can find that, in any case, a smaller lattice constant results in a smaller magnetic Mn moment, and the form of this dependency is actually very similar for the Ca and Y compounds. But in both compounds, the dependence of the magnetic moment on the Mn-Mn distance varies strongly with the kind of magnetic order, i.e., the moments of the Fm states increase most strongly at larger lattice constants, while in the AFl ordering, the biggest changes are observed at smaller in-plane lattice parameters.

If we compare the local Mn density of states of the in-plane ferromagnetic and antiferromagnetic structures of YMn_2Ge_2 and $CaMn_2Ge_2$, we realize that antiferromagnetic order results in narrower d bands and correspondingly larger magnetic moments (cf. Table I). In the ferromagnetic state, the majority and minority bands overlap significantly and an

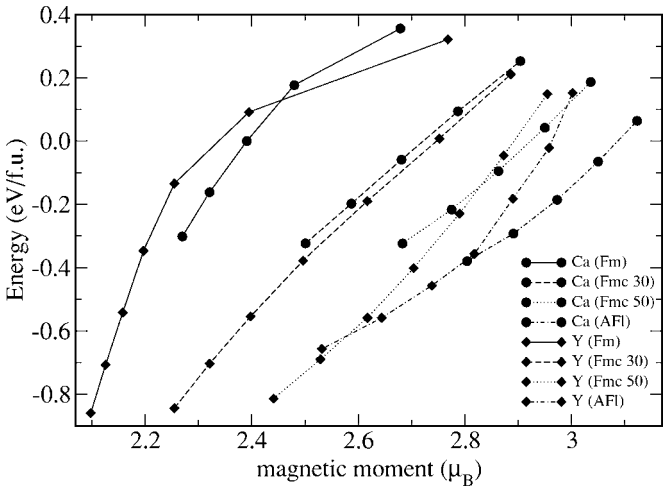

FIG. 4. Total energy of different magnetic configurations for $CaMn_2Ge_2$ (circles) and YMn_2Ge_2 (diamonds) as a function of the local Mn magnetic moments. The energies were normalized to the Fm state at experimental volume with an additional constant shift of −0.87 eV added to the energies of the Y phases. The magnetic moments of the Y compound have been obtained from in-plane lattice constants between 3.99 and 4.21 Å (cf. Fig. 2), while the lattice constant in the Ca compound has been varied between 4.06 and 4.23 Å (Fig. 3).

increase in the in-plane lattice constant leads to a quick destabilization of the Fm state accompanied by a modest increase in magnetic moment (cf. Fig. 4). In contrast, in the antiferromagnetic state, the Mn d electrons are already considerably more localized and a separation of minority and majority bands (i.e., an increase of magnetic moment) results in an only moderate increase of total energy. For intermediate cases, the Fmc structures at various canting angles show a gradual variation between the two extreme cases, the Fm and the AFl state. As can be seen from Fig. 4, this behavior does not depend very sensitively on the type of ions in the unit cell, but it seems to be a property of the Mn sublattice alone.

V. CONCLUDING REMARKS

We have made a systematic study of the ground-state phase diagram of $La_{1-x}Y_xMn_2Ge_2$ and $La_{1-x}Ca_xMn_2Ge_2$ by comparing total energies of a variety of magnetic structures of YMn_2Ge_2 and $CaMn_2Ge_2$ as a function of the in-plane lattice constant to simulate alloying with La.

We could reproduce with our calculations the experimental ground-state structures for the two considered series of alloys. The difference in the chemical valency of Y and Ca does not lead to large modifications in the magnetic moments of the Mn sublattice. These moments are mainly determined by the Mn-Mn distance, which is given by the size of the Y or Ca cations and by the in-plane magnetic coupling. This in-plane magnetic coupling and, thereafter, the features of the magnetic structure are indeed being influenced by the valency and electropositivity of the cations, which determine the number of conduction electrons in the interstitial region. For the same Mn-Mn in-plane distance, the stable magnetic phase is different for Ca and Y, even if the values of the corresponding Mn magnetic moments are similar. This confirms our above-mentioned conclusions.

Through the comparison of total energies for many different magnetic configurations as a function of Mn-Mn intraplane distance in the case of YMn_2Ge_2, we could see that there exists a critical distance D_C equal to 2.86 Å, below which the Mn atoms couple ferromagnetically, while for larger distances an in-plane antiferromagnetic component appears, giving rise to canted ground states. Hence, the occurrence of ferro- or antiferromagnetic in-plane components is obviously correlated to the $d_{\text{Mn-Mn}}$ spacings. It is noteworthy that the value found for D_C is close to the one proposed by Venturini *et al.*[3] (D_C=2.84 Å) and even closer to the one proposed by Goodenough[16] (D_C=2.85 Å), a value at which the 3d electrons of the Mn atom change their character from itinerant to localized.

Our calculations also show that if the R atom is divalent (+II), then the lowest energy configuration is always in-plane and interplane antiferromagnetic (AFl), while the mixed configurations seem to appear only if the R atom is trivalent (+III). Therefore, the appearance of a canted magnetic structure (*namely, the occurrence of a ferromagnetic component*) is a critical phenomenon which seems to occur only within the R(+III) compounds. A similar preference of the AFI structure in divalent states has been observed in $EuMn_2X_2$ compounds at low temperatures.[2]

ACKNOWLEDGMENTS

This work was partially funded by UBACyT-X115, PICT 03-10698, and the German-Argentinian collaboration program DAAD-Fundación Antorchas. A.M.L. belongs to Consejo Nacional de Investigaciones Científicas y Técnicas CONICET (Argentina).

[1] E. Duman, M. Acet, I. Dincer, A. Elmali, and Y. Elerman, J. Magn. Magn. Mater. **309**, 40 (2007).
[2] M. Hofmann, S. J. Campbell, and A. V. J. Edge, Phys. Rev. B **69**, 174432 (2004).
[3] G. Venturini, B. Malaman, and E. Ressouche, J. Alloys Compd. **241**, 135 (1996).
[4] I. Ijjaali, G. Venturini, B. Malaman, and E. Ressouche, J. Alloys Compd. **266**, 61 (1998).
[5] S. Di Napoli, A. M. Llois, G. Bihlmayer, S. Blügel, M. Alouani, and H. Dreyssé, Phys. Rev. B **70**, 174418 (2004).
[6] R. Welter, I. Ijjaali, G. Venturini, E. Ressouche, and B. Malaman, J. Magn. Magn. Mater. **187**, 278 (1998).
[7] G. Venturini, R. Welter, E. Ressouche, and B. Malaman, J. Alloys Compd. **210**, 213 (1994).

[8] U. v. Barth and L. Hedin, J. Phys. C **5**, 1629 (1972).
[9] V. L. Moruzzi, J. F. Janak, and A. R. Williams, *Calculated Electronic Properties of Metals* (Pergamon, New York, 1978).
[10] M. I. Katsnelson and V. P. Antropov, Phys. Rev. B **67**, 140406(R) (2003).
[11] Ph. Kurz, F. Förster, L. Nordström, G. Bihlmayer, and S. Blügel, Phys. Rev. B **69**, 024415 (2004).
[12] E. Wimmer, H. Krakauer, M. Weinert, and A. J. Freeman, Phys. Rev. B **24**, 864 (1981); M. Weinert, E. Wimmer, and A. J. Freeman, *ibid.* **26**, 4571 (1982).
[13] C. Herring, in *Magnetism*, edited by G. Rado and H. Suhl (Academic, New York, 1966), Vol. 4.
[14] L. M. Sandratskii, Adv. Phys. **47**, 91 (1998).
[15] B. Malaman, G. Venturini, R. Welter, and E. Ressouche, J. Alloys Compd. **210**, 209 (1994).
[16] J. B. Goodenough, in *Magnetism and the Chemical Bond* (Wiley-Interscience, New York, 1966), p. 240.